Available online at www.sciencedirect.com
SCIENCE DIRECT®
Journal of Power Sources 123 (2003) 247–252
JOURNAL OF POWER SOURCES
www.elsevier.com/locate/jpowsour

$Li(Ni_{1/3}Co_{1/3}Mn_{1/3})O_2$ as a suitable cathode for high power applications

I. Belharouak [a,*], Y.-K. Sun [b], J. Liu [a], K. Amine [a]

[a] *Chemical Engineering Division, Argonne National Laboratory, 9700 South Cass Ave., Argonne, IL 60439, USA*
[b] *Department of Chemical Engineering, Hanyang University, Seoul 133-791, South Korea*

Received 17 March 2003; accepted 31 March 2003

Abstract

The electrochemical performance of the layered $Li(Ni_{1/3}Co_{1/3}Mn_{1/3})O_2$ material have been investigated as a promising cathode for a hybrid electric vehicle (HEV) application. A $C/Li(Ni_{1/3}Co_{1/3}Mn_{1/3})O_2$ cell, cycled between 2.9 and 4.1 V at 1.5 C rate, does not show any sign of capacity fade up to 100 cycles, whereas at the 5 C rate, a loss of only 18% of capacity is observed after 200 cycles. The $Li(Ni_{1/3}Co_{1/3}Mn_{1/3})O_2$ host cathode converts from the hexagonal to a monoclinic symmetry at a high state of charge. The cell pulse power capability on charge and discharge were found to exceed the requirement for powering a hybrid HEV. The accelerated calendar life tests performed on $C/Li(Ni_{1/3}Co_{1/3}Mn_{1/3})O_2$ cells charged at 4.1 V and stored at 50 °C have shown a limited area specific impedance (ASI) increase unlike $C/Li(Ni_{0.8}Co_{0.2})O_2$ based-cells. A differential scanning calorimetry (DSC) comparative study clearly showed that the thermal stability of $Li(Ni_{1/3}Co_{1/3}Mn_{1/3})O_2$ is much better than that of $Li(Ni_{0.8}Co_{0.2})O_2$ and $Li(Ni_{0.8}Co_{0.15}Al_{0.05})O_2$ cathodes. Also, DSC data of $Li(Ni_{1/3}Co_{1/3}Mn_{1/3})O_2$ cathode charged at 4.1, 4.3, and 4.6 V are presented and their corresponding exothermic heat flow peaks are discussed.

Keywords: Li-ion batteries; Cathode material; Layered structure; Hybrid electric vehicle; High power

1. Introduction

Since its introduction in 1990 [1], the rechargeable lithium-ion battery with high energy density and power capability has become an important power source for portable electronic devices, such as cellular phones and laptop computers and, more recently, hybrid electric vehicles (HEV) [2–4]. In the past four years, Argonne National Laboratory has been working on understanding the power fade mechanism in lithium-ion batteries using $Li(Ni_{0.8}Co_{0.2})O_2$ and $Li(Ni_{0.8}Co_{0.15}Al_{0.05})O_2$ cathodes. High power type 18650 cells that incorporate a $Li(Ni_{0.8}Co_{0.2})O_2$ positive electrode, graphite as a negative electrode, and a 1 M $LiPF_6$ (EC:DEC, 1:1) electrolyte were fabricated and investigated. After initial performance characterization, the cells were subjected to an elevated-temperature calendar and cycle life testing as well as safety characterization. New and aged cells were disassembled and portions of their electrodes were investigated to identify the sources of the impedance rise and the power fade. The results of the study have shown that the interfacial resistance at the cathode material plays a major role in the life of the cell [5–7]. The impedance increase is caused by a phase segregation at the surface of the cathode and a formation of a resistive $Li_xNi_{1-x}O$ film [8]. This phase is the result of the reduction of highly oxidizing and unstable tetravalent Ni^{4+} that are generated during the charge of the cathode. Therefore, there is a need to search for an alternative cathode material that is more stable during the charging process. $Li(Ni_{1/3}Co_{1/3}Mn_{1/3})O_2$ could be an alternative cathode to $Li(Ni_{0.8}Co_{0.2})O_2$ and could offer longer calendar life for HEV application. The amount of active nickel in this material is small and the total oxidation of Ni to tetravalent state takes place at 4.6 V [9,10]. In addition, Mn^{4+} cations in the structure play a stabilizing role, preventing a structural collapse during cycling. By considering these two factors, we should expect no phase segregation in the case of $Li(Ni_{1/3}Co_{1/3}Mn_{1/3})O_2$ system within the voltage window 3–4.2 V. Therefore, we investigated the high power characteristics of $Li(Ni_{1/3}Co_{1/3}Mn_{1/3})O_2$ material as well as its thermal stability for HEV application.

* Corresponding author. Tel. +1-630-252-4450; fax: +1-630-252-4176.
E-mail address: belharouak@cmt.anl.gov (I. Belharouak).

0378-7753/$ – see front matter © 2003 Elsevier Science B.V. All rights reserved.
doi:10.1016/S0378-7753(03)00529-9

2. Experimental

$Li(Ni_{1/3}Co_{1/3}Mn_{1/3})O_2$ was made by mixed hydroxide method according to a preparation procedure previously reported by Shaju et al. [11]. The layered structure of the material was determined by X-ray diffraction (XRD) and its composition was confirmed by ICP analysis.

Positive electrodes were made by coating a paste of $Li(Ni_{1/3}Co_{1/3}Mn_{1/3})O_2$ active material, super-P carbon as a conducting additive, and polyvinylidene fluoride (PVdF) binder (80:10:10 (wt.%)) on an aluminum foil collector. The loading amount of the active material was 5–6 mg/cm^2. The electrolyte was 1.2 M $LiPF_6$ in a (1:1:3 (wt.%)) mixture of ethylene carbonate (EC), polycarbonate (PC), and dimethyl carbonate (DMC). The negative electrode was prepared by mixing graphite with 10 wt.% PVdF binder; the resulting paste was coated on copper foil. The cells were assembled inside a helium-filled dry-box and were evaluated using coin-type cells (CR2032: 1.6 cm^2). The charge–discharge measurements were carried out between 2.9 and 4.1 V potential range at current density of 0.1–1.25 mA/cm^2.

A hybrid pulse power characteristic (HPPC) test was applied on cells (32 cm^2 test fixture, 15.5 cm^2 effective surface) in accordance with the Partnership for a New Generation of Vehicles (PNGV) Battery Test Manual [12]. The test is intended to establish: (1) the discharge power capability at the end of an 18 s discharge current; and (2) the cell regeneration power capability over 2 s of a regeneration current pulse as a function of depth of discharge (DOD).

Accelerated aging tests were carried out on C/$Li(Ni_{1/3}Co_{1/3}Mn_{1/3})O_2$ cells. The cells were charged up to 4.1 V and kept in an oven at 50 °C. The area specific impedance (ASI) of the cells was monitored during storage. Similar accelerated aging tests were carried out on a conventional $Li(Ni_{0.8}Co_{0.2})O_2$ cathode using similar cell chemistry for the purpose of comparing its stability to that of the $Li(Ni_{1/3}Co_{1/3}Mn_{1/3})O_2$ cathode. Differential scanning calorimetry (DSC) measurements were also performed on $Li(Ni_{1/3}Co_{1/3}Mn_{1/3})O_2$ electrodes that were charged at 4.1, 4.3, and 4.6 V. Similarly, the thermal stability of $Li(Ni_{0.8}Co_{0.2})O_2$ and $Li(Ni_{0.8}Co_{0.2}Al_{0.05})O_2$ cathodes charged at 4.3 V were investigated by DSC and compared with that of $Li(Ni_{1/3}Co_{1/3}Mn_{1/3})O_2$.

3. Results and discussion

The powder X-ray diffraction pattern of $Li(Ni_{1/3}Co_{1/3}Mn_{1/3})O_2$ is shown in Fig. 1a. The observed diffraction lines can be indexed according to $R\bar{3}m$ space group of α-$NaFeO_2$ structure. The hexagonal lattice parameters, $a = 2.862$ Å and $c = 14.238$ Å, were refined using a Rietveld profile matching refinement option [13], and are consistent with the values published by Ohzuku et al. [9]. The 3d metals Ni, Co, and Mn are supposed to be randomly distributed on the (3b) crystallographic position, whereas the lithium atoms occupy the (3a) sites between the metallic slabs. Fig. 1b shows the X-ray diffraction (XRD) pattern of $Li(Ni_{1/3}Co_{1/3}Mn_{1/3})O_2$ charged at 4.6 V at a low rate (C/50). We noticed three major differences compared to the $Li(Ni_{1/3}Co_{1/3}Mn_{1/3})O_2$ discharged electrode: (1) the (0 0 6) line disappears from the XRD of de-intercalated $Li_\varepsilon Ni_{1/3}Co_{1/3}Mn_{1/3}O_2$ electrode; (2) the (1 0 8) and (1 1 0) peaks are clearly separated by 2° (2θ) instead of being

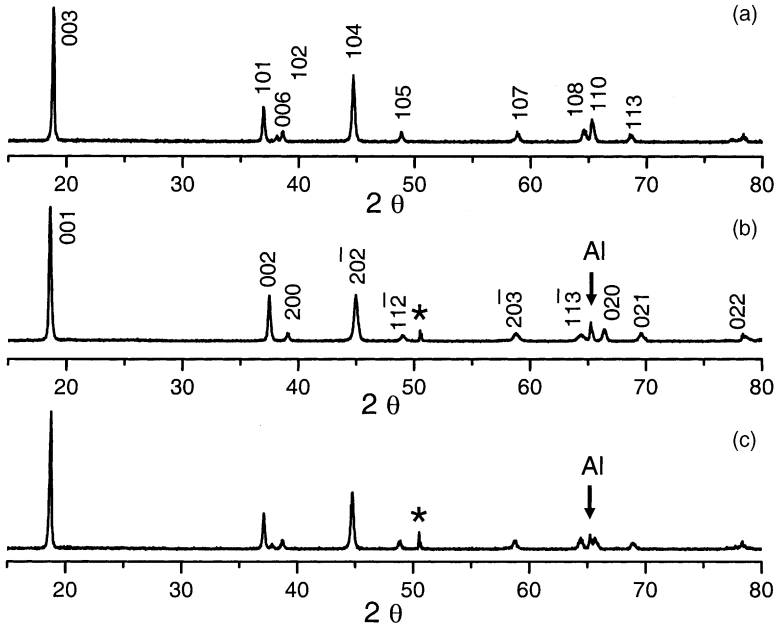

Fig. 1. X-ray diffraction patterns of: (a) $Li(Ni_{1/3}Co_{1/3}Mn_{1/3})O_2$ as-prepared; (b) $Li(Ni_{1/3}Co_{1/3}Mn_{1/3})O_2$ charged at 4.6 V; (c) $Li(Ni_{1/3}Co_{1/3}Mn_{1/3})O_2$ recuperated at discharged state after 200 charge/discharge cycles at 5 C rate. (✱) Sample holder; (↓) current collector.

barely split in the pristine cathode (Fig. 1a); (3) the (1 1 3) line is shifted toward the high 2θ angles. To understand these observations, we adopted the following strategy. First, a method for the automatic indexing of powder diffraction patterns (Dicvol [14]) was used. The best result corresponded to a monoclinic symmetry. More recently, Arachi et al. [15] confirmed the monoclinic symmetry for an electrochemically de-intercalated $Li_\varepsilon Ni_{0.5}Mn_{0.5}O_2$ by XRD and transmission electron microscopy (TEM). For instance, the X-ray pattern of $Li_{0.5}Ni_{0.5}Mn_{0.5}O_2$ exhibits notable similarities to that of $Li_\varepsilon Ni_{1/3}Co_{1/3}Mn_{1/3}O_2$ shown in Fig. 1b. Therefore, we adopted the monoclinic system as the most likely symmetry for the charged $Li(Ni_{1/3}Co_{1/3}Mn_{1/3})O_2$ cathode. The best fit of the crystalline parameters leads to the following unit cell parameters: $a = 4.906$ Å, $b = 2.824$ Å; and $c = 5.084$ Å, $\beta = 108.35^\circ$ with the space group $C2/m$. Although the exact atomic position of this charged cathode is still unknown, it is inferred that a lithium-vacancies ordering is what causes the reduction of symmetry from hexagonal to monoclinic. The details of a complete crystallographic study will be published elsewhere. Fig. 1c presents the XRD pattern of an intercalated $Li(Ni_{1/3}Co_{1/3}Mn_{1/3})O_2$ electrode after 200 cycles at 5 C rate. The result shows mainly that $Li(Ni_{1/3}Co_{1/3}Mn_{1/3})O_2$ maintains its crystallinity and layered structure, unlike $Li(Ni_{0.8}Co_{0.2})O_2$, where peaks broaden after extensive cycling. The retention of the crystallinity of the $Li(Ni_{1/3}Co_{1/3}Mn_{1/3})O_2$ cathode even at a very high rate of full charge and discharge could help expand the life of a battery based on this system.

The electrochemical performances of $Li/Li(Ni_{1/3}Co_{1/3}Mn_{1/3})O_2$ cells have been preliminarily evaluated to quantity the specific capacity. $Li/Li(Ni_{1/3}Co_{1/3}Mn_{1/3})O_2$ cell initially delivers a discharge capacity of over 200 mAh/g between 2.9 and 4.6 V at a current density of 0.1 mA/cm^2 as shown in Fig. 2.

Fig. 3 shows the discharge capacities versus cycle number of $C/Li(Ni_{1/3}Co_{1/3}Mn_{1/3})O_2$ coin cells at 1.5 and 5 C rates, respectively. The cell cycled at 1.5 C rate maintains its capacity up to 100 cycles (Fig. 3a), whereas the cell operating at a higher rate (5 C) shows only 18% loss of capacity after 200 cycles (Fig. 3b). The HPPC tests were carried out on $C/Li(Ni_{1/3}Co_{1/3}Mn_{1/3})O_2$ cells using a 10 C pulse rate. Fig. 4 presents the area specific impedance (ASI) for the 18 s pulse discharge and 2 s regenerative charge as a function of depth of discharge (DOD). The ASI values are lower than those calculated from the Argonne National Laboratory (ANL) battery design spreadsheet model for a 25 kW battery pack, which are 35 Ω cm^2 for an 18 s discharge and 25 Ω cm^2

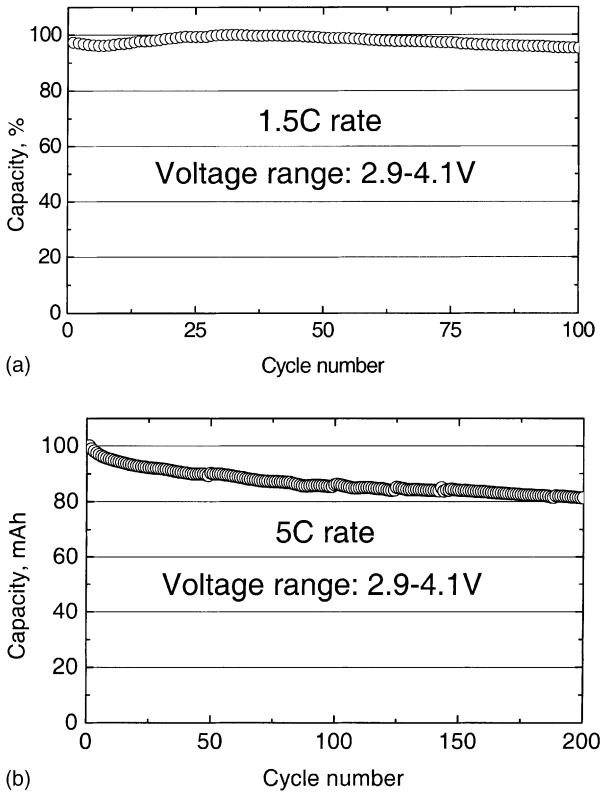

Fig. 3. Discharge capacity vs. number of cycles of $C/Li(Ni_{1/3}Co_{1/3}Mn_{1/3})O_2$ cells cycled between 2.9 and 4.1 V at room temperature under: (a) 1.5 C, and (b) 5 C rates.

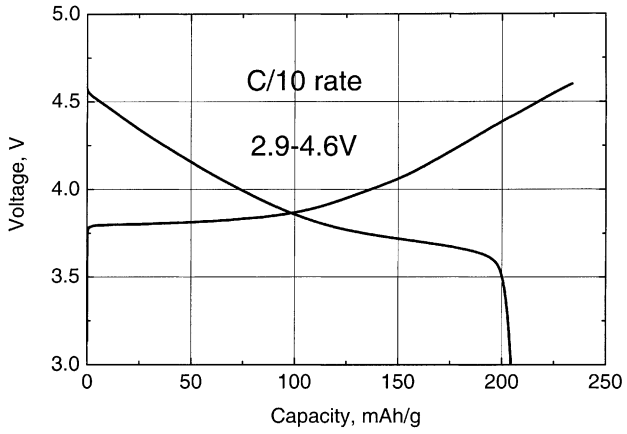

Fig. 2. Voltage profile of $Li/Li(Ni_{1/3}Co_{1/3}Mn_{1/3})O_2$ cell cycled between 3.0 and 4.6 V at a current density of 0.1 mA/cm^2.

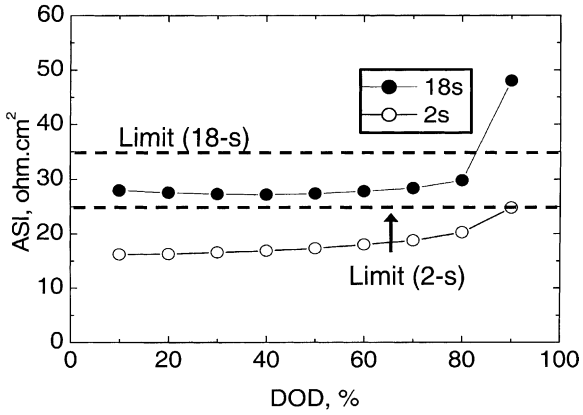

Fig. 4. Pulse power ASI as a function of DOD for a $C/Li(Ni_{1/3}Co_{1/3}Mn_{1/3})O_2$ cell.

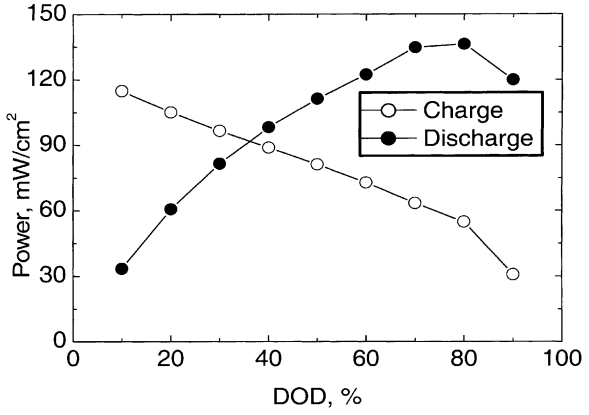

Fig. 5. Charge and discharge pulse power capability as a function of DOD for a C/Li($Ni_{1/3}Co_{1/3}Mn_{1/3}$)O_2 cell.

for a 2 s charge pulse. Fig. 5 shows the corresponding pulse power characteristics of the C/Li($Ni_{1/3}Co_{1/3}Mn_{1/3}$)O_2 cell. The pulse power at each DOD is calculated from the ASI and the cell open circuit voltage [6]. The test is used to determine the total available state of charge and energy swings that can be utilized within the HEV operating voltage limits for specified discharge power and regeneration levels. We found that the cells meet the power requirement especially in the "sweet spot" of 30–70% DOD. To meet the power requirement for HEV, the model mentioned above predicts the power of 66 mW/cm^2 for the 2 s regeneration charge, and 55 mW/cm^2 for the 18 s pulse. These values were easily exceeded in the C/Li($Ni_{1/3}Co_{1/3}Mn_{1/3}$)O_2 system between 30 and 70% DOD as shown in Fig. 5. This result clearly indicates that a battery based on C/Li($Ni_{1/3}Co_{1/3}Mn_{1/3}$)O_2 can meet and exceed the power requirement for the HEV application.

Fig. 6 shows the result of an accelerated aging test of C/Li($Ni_{1/3}Co_{1/3}Mn_{1/3}$)O_2 and C/Li($Ni_{0.8}Co_{0.2}$)O_2 cells charged at 4.1 V. The ASI of the C/Li($Ni_{0.8}Co_{0.2}$)O_2 cell is 45 Ω cm^2 in the beginning of the experiment and reaches

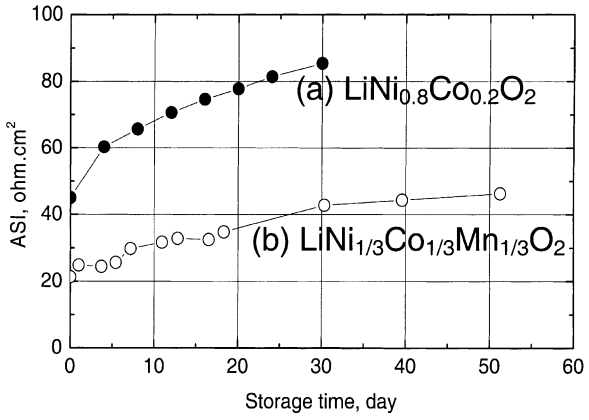

Fig. 6. Accelerated aging tests of cells made of: (a) a C/Li($Ni_{1/3}Co_{1/3}Mn_{1/3}$)O_2 cell; and (b) a C/Li($Ni_{0.8}Co_{0.2}$)O_2 cell. The cells were systematically charged at 4.1 V and stored at 50 °C.

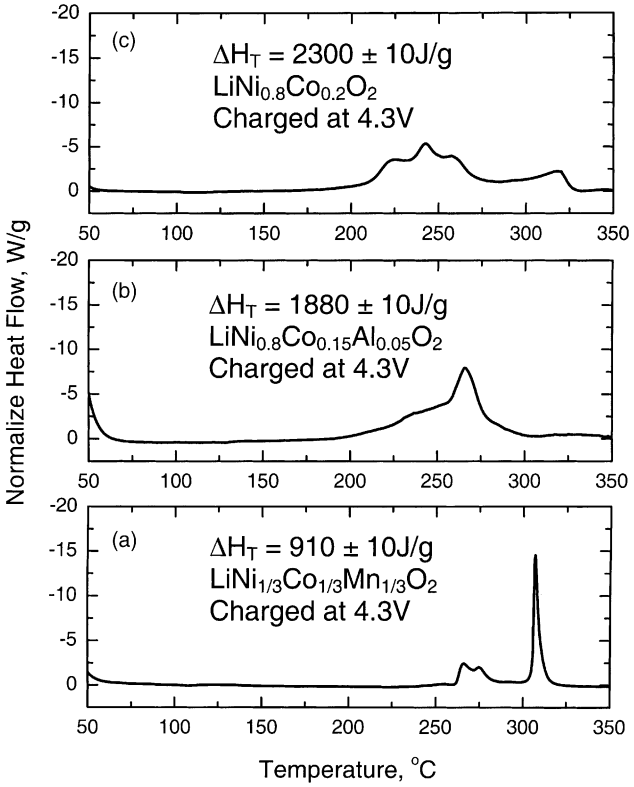

Fig. 7. DSC measurement of cathodes charged at 4.3 V: (a) Li($Ni_{1/3}Co_{1/3}Mn_{1/3}$)O_2; (b) Li($Ni_{0.8}Co_{0.15}Al_{0.05}$)$O_2$; (c) Li($Ni_{0.8}Co_{0.2}$)$O_2$.

85 Ω cm^2 only after 30 days storage at 50 °C. However, the C/Li($Ni_{1/3}Co_{1/3}Mn_{1/3}$)O_2 cell shows much lower ASI values in the beginning (22 Ω cm^2) with very limited increase in the ASI after 50 days of accelerated aging. This result clearly indicates that Li($Ni_{1/3}Co_{1/3}Mn_{1/3}$)O_2 is more stable than Li($Ni_{0.8}Co_{0.2}$)O_2 and could offer much longer calendar life if incorporated in high power cell design.

Differential scanning calorimetry (DSC) measurements were performed on Li($Ni_{1/3}Co_{1/3}Mn_{1/3}$)O_2, Li($Ni_{0.8}Co_{0.2}$)O_2, and Li($Ni_{0.8}Co_{0.15}Al_{0.05}$)$O_2$ electrodes charged at 4.3 V; results are shown in Fig. 7. Li($Ni_{0.8}Co_{0.2}$)O_2 and Li($Ni_{0.8}Co_{0.15}Al_{0.05}$)$O_2$ exhibit at least three broad exothermic peaks between 200 and 300 °C. Although they start reacting with the electrolyte at the edge of 200 °C, the total heat generated by Li($Ni_{0.8}Co_{0.2}$)O_2 (2300 J/g) is much greater than that produced by Li($Ni_{0.8}Co_{0.15}Al_{0.05}$)$O_2$ (1880 J/g). The DSC curve of Li($Ni_{1/3}Co_{1/3}Mn_{1/3}$)O_2 is different and consists of three sharp exothermic peaks: a pair of 2 weak peaks centered at 265 and 275 °C with an onset temperature of 260 °C, and a third isolated peak at 305 °C with an onset temperature of 300 °C. The total heat associated with the three exothermic peaks is estimated at 910 J/g, which is much lower than the heat generated by the Li($Ni_{0.8}Co_{0.15}Al_{0.05}$)$O_2$. These results clearly show that the Li($Ni_{1/3}Co_{1/3}Mn_{1/3}$)O_2 cathode has better thermal stability characteristics than either Li($Ni_{0.8}Co_{0.2}$)O_2 cathode or its stabilized form Li($Ni_{0.8}Co_{0.15}Al_{0.05}$)$O_2$. Fig. 8

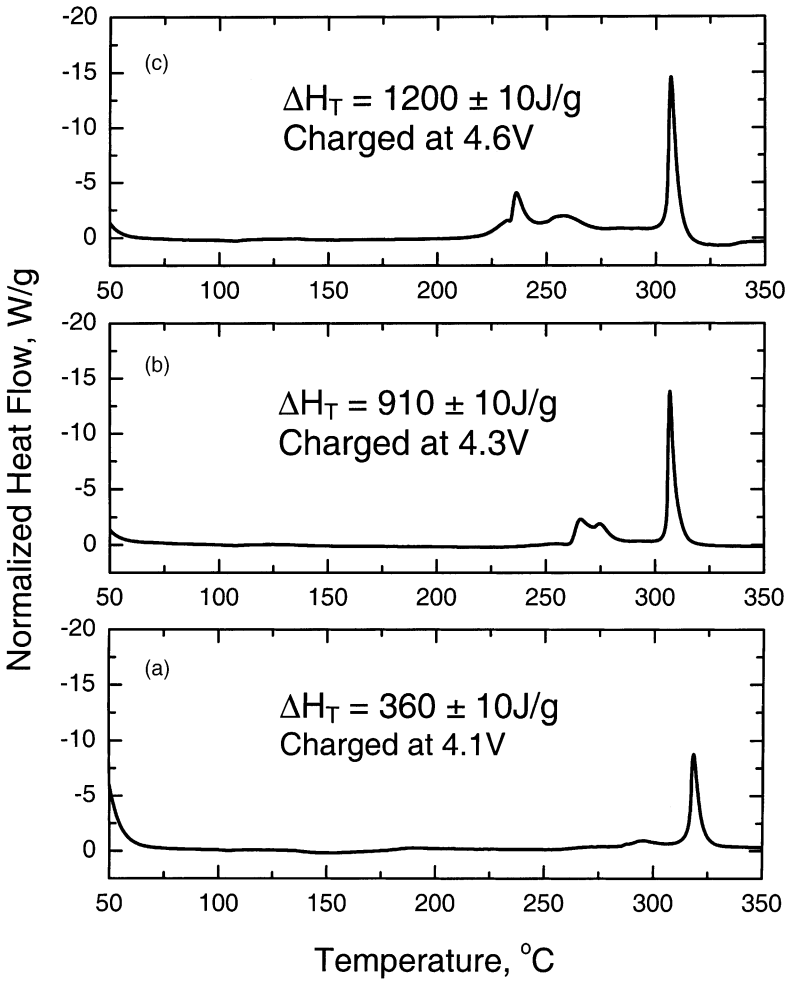

Fig. 8. DSC measurement of $Li(Ni_{1/3}Co_{1/3}Mn_{1/3})O_2$ positive electrode charged at: (a) 4.1 V, (b) 4.3 V and (c) 4.6 V.

represents the DSC data of the $Li(Ni_{1/3}Co_{1/3}Mn_{1/3})O_2$ electrode charged at 4.1, 4.3, and 4.6 V. For the electrode charged at 4.1 V, one major peak at 318 °C (onset temperature of 310 °C) is observed, with a barely visible broad peak centered at around 295 °C. The electrode charged at 4.6 V displays a DSC pattern similar to the electrode charged at 4.3 V, with the small peak shifted to a much lower temperature (225–275 °C). The total generated heats are 360, 910, and 1200 J/g for the electrode charged at 4.1, 4.3, and 4.6 V, respectively. This clearly reveals that the stability of the $Li(Ni_{1/3}Co_{1/3}Mn_{1/3})O_2$ electrode decreases with the increase in the ratio of the delithiation of the cathode. Nevertheless, $Li(Ni_{1/3}Co_{1/3}Mn_{1/3})O_2$ charged at 4.6 V is much safer than both the conventional $Li(Ni_{0.8}Co_{0.2})O_2$ and $Li(Ni_{0.8}Co_{0.15}Al_{0.05})O_2$ cathodes charged at 4.3 V.

4. Conclusions

$Li(Ni_{1/3}Co_{1/3}Mn_{1/3})O_2$, prepared by a mixed hydroxide method, has shown outstanding electrochemical performances. It delivers a high discharge capacity of over 200 mAh/g between 3.0 and 4.6 V, and shows excellent cyclability even at the 5 C rate without changing the crystallinity of the cathode. The high power pulse characteristics (HPPC) of the cell can meet and exceed the requirements established for the hybrid electric vehicle application. The accelerated aging test of $C/Li(Ni_{1/3}Co_{1/3}Mn_{1/3})O_2$ cells charged at 4.1 V and stored at 50 °C up to 50 days shows that the $Li_{1-x}(Ni_{1/3}Co_{1/3}Mn_{1/3})O_2$ cathode is more suitable for lithium-ion batteries in the HEV application. The DSC measurements confirm that a $Li(Ni_{1/3}Co_{1/3}Mn_{1/3})O_2$ cathode has better thermal safety characteristics than those of the conventional $Li(Ni_{0.8}Co_{0.2})O_2$ and $Li(Ni_{0.8}Co_{0.15}Al_{0.05})O_2$ cathodes.

Acknowledgements

This work was supported by the US Department of Energy, Office of Advanced Automotive Technologies, under Contract no. W-31-10-ENG-38.

References

[1] T. Nagaura, K. Tozawa, Prog. Batteries Solar Cells 9 (1990) 209.
[2] K. Amine, J. Liu, ITE Lett. 1 (2000) 59.
[3] A.M. Andersson, D.P. Abraham, R. Haasch, S. MacLaren, J. Liu, K. Amine, J. Electrochem. Soc. 149 (2002) A1358.
[4] K. Amine, C.H. Chen, J. Liu, M. Hammond, A. Jansen, D. Dees, I. Bloom, D. Vissers, G. Henriksen, J. Power Sources 97–98 (2001) 684.
[5] M. Balasubramanian, X. Sun, X.Q. Yang, J. McBreen, J. Power Sources 92 (2001) 1.
[6] I. Bloom, B.W. Cole, J.J. Sohn, S.A. Jones, E.G. Polzin, V.S. Battaglia, G.L. Henriksen, C. Motlock, R. Richardson, J. Power Sources 101 (2001) 238.
[7] X. Zhang, P.N. Ross Jr., R. Kostecki, F. Kong, S. Sloop, J.B. Kerr, K. Striebel, E.J. Cairns, F. McLarnon, J. Electrochem. Soc. 148 (2001) A463.
[8] D.P. Abraham, R.D. Twesten, M. Balasubramanian, I. Petrov, J. McBreen, K. Amine, Electrochem. Comm. 4 (2002) 620.
[9] T. Ohzuku, Y. Makimura, Chem. Lett. 7 (2001) 642.
[10] N. Yabuuchi, T. Ohzuku, Extended Abstract No. 122, IMLB11, Monterey, USA, 23–28 June 2002.
[11] K.M. Shaju, G.V. Subba Rao, B.V.R. Chowdari, Electrochem. Acta 48 (2002) 145.
[12] PNGV Battery Test Manual, Revision 1, Idaho National Engineering Laboratory, Department of Energy, DOE/ID-10597, August 1999.
[13] J. Rodriguez-Carvajal, in: Proceedings of the Powder Diffraction Satellite Meeting of the XVth Congress of IUCr, Abstract, Toulouse, 1990, p. 127.
[14] A. Boultif, D. Louer, J. Appl. Crystallogr. 24 (1991) 987.
[15] Y. Arachi, H. Kobayashi, S. Emura, Y. Nakata, M. Tanaka, T. Asai, Chem. Lett. 32 (1) (2003) 60.